# First endemic freshwater *Gammarus* from Crete and its evolutionary history – an integrative taxonomy approach

3    Kamil Hupało[1], Tomasz Mamos[1], Weronika Wrzesińska[1], Michał Grabowski[1]

4    Department of Invertebrate Zoology and Hydrobiology, University of Lodz, Lodz, Poland

6    Corresponding Author:

7    Kamil Hupało

8    Banacha 12/16, Lodz, 90-237, Poland

9    Email address: kamilhupalo@gmail.com

25    **Abstract**:

26    The Mediterranean islands are known as natural laboratories of evolution with a high level of

27    endemic biodiversity. However, most biodiversity assessments have focused mainly on terrestrial

28    and marine fauna, leaving the freshwater animals aside. Crete is one of the largest islands in the

29    Mediterranean Basin, with a long history of isolation from the continental mainland. Gammarid

30    amphipods are often dominant in macrozoobenthic communities in European inland waters.

31    They are widely used in biomonitoring and exotoxicological studies. Herein, we describe

32    ***Gammarus plaitisi* sp. nov.**, endemic to Cretan streams, based on morphological characters and

33    a set of molecular species delimitation methods using mitochondrial cytochrome oxidase subunit

34    I and 16S rRNA genes as well as   nuclear 28S rDNA, ITS1 and EF1-alpha genes. The

35    divergence of the new species is strongly connected with the geological history of the island

36    supporting its continental origin.

37    **Introduction**

38    Due to its complex geological history and unique combination of geological and climatic factors,

39    the Mediterranean Region is recognized as one of the globally most important hotspots of

40    biodiversity and endemism, and is a model system for studies of biogeography and evolution

41    (Woodward 2009, Poulakakis et al. 2014). The freshwater fauna of the region is still heavily

42    understudied, yet it is estimated that the Mediterranean is inhabited by ca. 35% of  Palearctic

43    species, which mean the region contains more than 6% of the world's freshwater species.At least

44    43% of the freshwater Mediterranean species are considered to be local endemics (Figueroa et al.

45    2013). Most of these endemics occupy the Mediterranean islands (Myers et al. 2000, Whittaker

46    & Fernández-Palacios 2007).

47    Crete is the fifth largest of the Mediterranean islands and the largest of the Aegean islands. At

48    the beginning of the Miocene, Crete was a part of the mainland composed of the Balkan

49    Peninsula and Asia Minor (23-12 million years ago). Around 12 million years ago, the split of

50    the Balkan Peninsula (including Crete) from Asia Minor began. Afterwards, about 11-8 million

51    years ago, the isolation of Crete from Peloponnesus started, due to the rise of sea levels. Later,

52  between 5.96 and 5.33 million years ago, the dessication of the Proto-Mediterranean Sea during
53  the Messinian Salinity Crysis led to the formation of hypersaline deserts around Crete and other
54  islands, and this is the last known land connection between Crete and the mainland (Poulakakis
55  et al. 2014). During the Pliocene, Crete was divided temporarily into at least four islands due to
56  sea level rise associated with the Zanclean flood (Sondaar & Dermitzakis 1982). At the end of
57  the Pliocene or in the Early Pleistocene, Crete gained  its present configuration.

58  Gammarid amphipods are among the most speciose, abundant and biomass-dominant, groups of
59  benthic macroinvertebrates in lotic ecosystems in Europe and, particularly, in the Mediterranean
60  Region (Macneil et al. 1997). They are also considered to be aquatic keystone species,
61  structuring freshwater macroinvertebrate communities (Kelly et al. 2002). They are widely used
62  as model organisms in biomonitoring and exotoxicological studies (i.e. Neuparth et al. 2002,
63  2005, Kunz et al. 2010). Gammarids are considered to be very good evolutionary models as they
64  are exclusively aquatic organisms with limited dispersal abilities (Bilton et al. 2001). The
65  majority of studies upon biodiversity of  Mediterranean amphipods have focused exclusively on
66  marine species, leaving the freshwater fauna relatively poorly known. So far, around 120
67  freshwater gammarid species living in the Mediterranean have been described ,  while only 15
68  species of two genera: *Gammarus* Fabricius, 1775 and *Echinogammarus* Stebbing, 1899, have
69  been reported from the islands (Karaman & Pinkster 1977, Pinkster 1993). Recently, an
70  extraordinarily high rate of cryptic diversity was discovered within several morphospecies from
71  both mentioned genera (Hou et al. 2011, 2014, Weiss et al. 2014, Wysocka et al. 2014, Mamos et
72  al. 2014, 2016; Copilaș-Ciocianu and Petrusek 2015, 2017; Katouzian et al. 2016, Grabowski et
73  al. 2017a,b). One can conclude that the number of species already reported from the
74  Mediterranean islands is definitely underestimated. Moreover, molecular studies on  insular
75  species are absent. To date, there have been two freshwater endemic species reported from Crete,
76  *E. kretensis* and *E. platvoeti*, both described by Pinkster (1993). As well, *Gammarus pulex pulex*
77  (Linnaeus, 1758), a freshwater species widespread throughout Europe, has been reported from
78  one locality on Crete (Karaman 2003). No other insular freshwater *Gammarus* species has been
79  reported from the Mediterranean.

80  In this paper, we show evidence that the Cretan population of *Gammarus pulex pulex* is, in fact, a
81  new species and describe it as *Gammarus plaitisi* sp. nov., based on  morphological,

82  ultrastructural and molecular features. We also reconstruct, based on a multimarker dataset, the

83  phylogeny of this species with respect to other lineages of *G. pulex* to reveal its biogeographic

84  afiliations and possible origin.

85

86  **Materials and methods**

87  *Sample collection, identification and material deposition*

88  The study material was collected from seven out of 53 sampling sites, including springs, streams,

89  rivers and lakes, visited during two sampling campaigns to Crete in 2011 and 2015 (Fig.1).

90  Multihabitat sampling was done with rectangular kick sample nets (aperture 25x25 cm and 0.5

91  mm mesh size). The samples were sorted at the site and amphipods were immediately fixed in

92  96% ethanol. Afterwards, the material was evaluated with a Nikon 800 stereomicroscope.

93  Identification to species was done according to the diagnostic morphological characters

94  described by Karaman & Pinkster (1977a,b, 1987) and by Pinkster (1993). Selected adult

95  individuals were dissected and all the appendages of diagnostic value were stained with lignin

96  pink (Azophloxin, $C_{18}H_{13}N_3Na_2O_8S_2$) andmounted with Euparal (Carl Roth GmBH, 7356.1) on

97  microscope slides. Afterwards they were photographed and drawn according to the protocol

98  described by Coleman (2006, 2009). The body length of the specimens was measured along the

99  dorsal side of the body from the base of the first antennae to the base of the telson. All the

100 materials other than holotypes and paratypes are deposited in the collection of the Department of

101 Invertebrate Zoology & Hydrobiology of University of Lodz. The type material is deposited in

102 the Museum and Institute of Zoology Polish Academy of Sciences (catalogue numbers: MIZ

103 1/2018/1, MIZ 1/2018/2, MIZ 1/2018/3, MIZ 1/2018/4, MIZ 1/2018/5, MIZ 1/2018/6) and

104 Museum für Naturkunde in Berlin (catalogue number: ZMB 30868)). Relevant voucher

105 information and sequence trace files are accessible on the Barcode of Life Data Systems (BOLD;

106 Ratnasingham & Hebert, 2007). In addition, all the sequences were deposited in GenBank

107 (accession numbers: COI: MG784477 to MG784549; 16S: MG784344 to MG784406; 28S:

108 MG784423 to MG784456; ITS1: MG784460 to MG784476; EF1-α: MG792351 to MG792367).

109 The electronic version of this article in Portable Document Format (PDF) will represent a

110 published work according to the International Commission on Zoological Nomenclature (ICZN),

111 and hence the new name contained in the electronic version is effectively published under that

112   Code from the electronic edition alone. This published work and the nomenclatural acts it

113   contains have been registered in ZooBank, the online registration system for the ICZN. The

114   ZooBank LSIDs (Life Science Identifiers) can be resolved and the associated information viewed

115   through any standard web browser by appending the LSID to the prefix http://zoobank.org/. The

116   LSID   for   this   publication   is:   [urn:lsid:zoobank.org:pub:E7EA69BA-9A8E-4B44-B999-

117   C2BA7B69AC76]. The online version of this work is archived and available from the following

118   digital repositories: PeerJ, PubMed Central and CLOCKSS.

119   *Scanning Electrone Microscope analysis*

120   Individuals used for scanning electron microscope (SEM) analysis were critical point dried and

121   sputter-coated with colloidal gold (10 nm). Pictures were taken with a PHENOM PRO X SEM in

122   the Department of Invertebrate Zoology and Hydrobiology of University of Lodz. The

123   photographs of the composition of the pores on antenna 1 and epimeral plate 2 were taken from

124   three same-sized individuals belonging respectively to *G. plaitisi* sp. nov. and other populations

125   of *G. pulex pulex* under four different magnifications.

126   *DNA extraction, PCR amplification, sequencing, haplotype diversity and sequence analysis*

127   About 3 mm$^3$ of the muscle tissue was taken out from each individual, with a sharp-edged

128   forceps and incubated overnight at 55°C in a 1.5-ml tube containing 200 µl of Queen's lysis

129   buffer with 5 µl of proteinase K (20 mg ml$^{-1}$) (Seutin et al. 1991). Total DNA was extracted

130   using the standard phenol/chlorophorm method (Hillis et al. 1996). Air-dried DNA pellets were

131   resuspended in 100 µl of TE buffer, pH 8.00, stored at 4°C until amplification and finally

132   longterm stored at -20°C. At first, 57 individuals from 7 sampling sites were barcoded for cox I

133   gene fragment using LCO1490/HCO2198 (Folmer et al. 1994) and LCO1490-JJ and HCO2198-

134   JJ (Astrin and Stüben 2011). PCR settings for amplifying COI sequences consisted of initial

135   denaturing of 60s at 94°C, five cycles of 30 s at 94 °C, 90 s at 45°C, 60 s at 72°C, then 35 cycles

136   of 30 s at 94°C, 90 s at 51°C, 60 s at 72°C, and final 5 min extension at 72°C (Hou et al. 2007).

137   The cleaning of the PCR products was done with exonuclease I (20 U mL-1, Fermentas) and

138   alkaline phosphatase FastAP (1 U mL-1, Fermentas) treatment according to the manufacturer's

139   guidelines. Subsequently, the products have been sequenced using the same primers as at the

140   amplification stage. Sequencing of the PCR products was performed using BigDye terminator

141   technology by Macrogen Inc.

142    All resulting sequences were verified and confirmed as *Gammarus* DNA via BLASTn searches

143    in GenBank (Altschul et al. 1990) and then assembled and aligned in Geneious software (Kearse

144    et al. 2012). The alignment was performed using MAFFT plugin with G-INS-i algorithm in

145    Geneious software (Katoh et al. 2002).

146    The DNAsp software (Librado and Rozas 2009) was used to define the haplotypes and to

147    calculate the haplotype and nucleotide diversity. The intraspecific pairwise genetic distances

148    were calculated in MEGA7 software (Kumar et al. 2016). The relationships between haplotypes

149    were illustrated with median-joining network (Bandelt et al. 1999) in PopArt (Leigh and Bryant

150    2015).

151    Additional COI sequences of closely related lineages from Greece and Sweden (geographically

152    nearest to type locality of *G. pulex pulex*), and outgroup *Gammarus* species were downloaded

153    from NCBI GenBank and added to analyses to test the monophyly of *G.*cf *pulex* group. (Tab.1).

154    The neighbour-joining tree of all COI sequences, using Tamura-Nei model of evolution with

155    1,000 bootstrap replicates, was created in MEGA7 software (Kumar et al. 2016).

156    Afterwards, at least three individuals per each delimited cluster were amplified for one additional

157    mitochondrial and two nuclear markers for phylogeny reconstruction: 1) mitochondrial 16S

158    rRNA using 16STf and 16SBr markers (Palumbi et al. 1991, MacDonald et al. 2005) under the

159    following PCR conditions: initial denaturation at 94°C for 150 s; 36 cycles of denaturation at

160    94°C for 40 s, annealing at 54°C for 40 s, extension at 65°C for 80 s; and a final extension at

161    65°C for 8 min (Weiss et al. 2014); 2) the nuclear 28S rRNA gene amplified with 28F and 28R

162    primers (Hou et al. 2007) under following conditions: initial denaturation at 94°C for 3min, 35

163    cycles of denaturation at 94°C for 20s, annealing at 55°C for 45s, and elongation at 65°C for 60s,

164    followed by a final extension for 2min at 65°C and 5 min extension at 72°C; 3) the nuclearITS1

165    gene with ITS1F and ITS1R primers (Chu et al. 2001) under following PCR conditions: 90

166    seconds at 94°C, 33 cycles of 20 seconds at 94°C, 30 seconds at 56.8°C, and 30 seconds at 72°C,

167    and finally 5 minutes at 72°C and EF1-α gene using EF1a-F and EF1a-R primers (Hou et al.

168    2011) under following PCR conditions: 60 s at 94°C, followed by 35 cycles of 30 s at 94°C, 45 s

169    at 45–50°C, 60 s at 72°C, and 5 min extension at 72°C. The nuclear markers were sequenced in

170    both directions.

171    *MOTU delimitation – cryptic diversity*

172 The Molecular Operational Taxonomic Units (MOTUs) were delimited, based on the COI
173 marker, with five methods and two different approaches (as done before by Grabowski et al.
174 2017b): the distance-based approaches, namely Barcode Index Number (BIN) System
175 (Ratnasingham & Hebert, 2013) and barcode gap discovery with the ABGD software (Puillandre
176 et al., 2012) and the tree-based approaches, using two GMYC model-based methods (Pons et al.,
177 2006) according to Monaghan et al. (2009) and the bPTP procedure described by Zhang et al.
178 (2013).

179 The BIN method is a distance-based approach, embedded in the Barcode of Life Data systems
180 (BOLD; Ratnasingham & Hebert, 2007). The sequences already deposited in BOLD database are
181 confronted with the newly submitted ones. Afterwards, according to their molecular divergence,
182 the sequences are clustered using algorithms that identify discontinuities between the clusters. A
183 unique and specific Barcode Index Number (BIN) is assigned to each cluster. If the submitted
184 sequences do not group together with already known BINs, a new number is created. Each BIN
185 is registered in BOLD database.

186 The Automated Barcode Gap Discovery (ABGD) method uses pairwise distance measures.
187 ABGD clusters the sequences into MOTUs (Molecular Operational Taxonomic Units), in the
188 way that the genetic distance between two sequences belonging to two separate groups will
189 always be greater than an indicated threshold (i.e. barcode gap). In our study, the primary
190 partitions were used as a principal for cluster delimitation, as they tend to remain stable on a
191 wider range of prior values, minimising the oversplitting of the number of groups and are usually
192 the closest to the number of taxa described by taxonomists (Puillandre et al., 2012). The default
193 value of 0.001 was applied as the minimum intraspecific distance. As the maximum intraspecific
194 distance we investigated a set of values up to 0.1, which has been proposed as suggested
195 maximum distance value in amphipods distinguishing two separate species (Costa et al., 2007).
196 The standard Kimura two-parameter (K2P) model correction was used (Hebert et al., 2003).

197 The bPTP approach for species delimitation is a tree based method, utilising non-ultrametric
198 phylogenies. The number of substitutions in incorporated into the model of speciation and the
199 bPTP assumes that the probability that a substitution leads to a speciation event follows a
200 Poisson distribution, as the lengths of the branches of the input tree are generated independently
201 according to either to speciation or coalescence, which are two classes of the Poisson processes.

202    In bPTP, the Bayesian support values are added for each delimited cluster (Zhang et al., 2013).

203    As an input tree, the phylogeny was generated using Bayesian inference in Geneious software

204    package using MrBayes plugin (Kearse et al. 2012) with MCMC chain 1 million iterations long,

205    sampled every 2,000 iterations. The TN93+I+G was chosen as the substitution model, as bestfit

206    based on bModel test (Bouckaert and Drummond 2017). The consensus tree was constructed

207    after removal of 25% burn-in phase. The analysis itself was done using the bPTP web server

208    (http://www.species.h-its.org/ptp/) with 500,000 iterations of MCMC and 10% burn-in.

209    The GMYC method identifies the transition from intraspecific branching patterns (coalescent) to

210    typical interspecific branching patterns (Yule processes) on an ultrametric, phylogenetic tree,

211    using the maximum likelihood approach. The estimation of the boundary between coalescent and

212    Yule branching processes can be done using two different GMYC approaches, one using the

213    single threshold and the second one based on multiple threshold model. We have reconstructed

214    an ultrametric tree, which is required for GMYC analyses, in BEAST software, using 20 million

215    iterations long MCMC chain, with TN93+I+G as the best-fit substitution model. The consensus

216    tree was analysed in the GMYC web server (available at: http://species.h-its.org/gmyc/) using

217    both the single and multiple threshold models.

218    *Time calibration and phylogeny reconstruction*

219    The time-callibrated phylogeny was reconstructed based on data from sequences of COI (586

220    bp), 16S rRNA (299 bp), 28S rRNA (781 bp), ITS1 (548 bp) and EF1-alpha (602 bp) in

221    BEAST2 software package (Bouckaert et al. 2014) with the use of five MCMC chains of

222    50 000 000 runs with following models of substitution: TN93+I+G (for COI), HKY+I+G (for

223    16S), TN93+I+G (for 28S), HKY+I+G (for ITS1) and TN93+I+G (for EF1-alpha) The models

224    for each marker were selected according to bModel test (Bouckaert and Drummond 2017). The

225    relaxed log-normal clock model was used and based on the selected rate of 0.0115 substitutions

226    (SD 0.0026) per million years for COI according to already established rate (Brower 1994),

227    which was cross-validated against two other rates (0.0113, 0.0127) established recently for other

228    freshwater members of *Gammarus*, in the *G. roeselii* species complex (Grabowski et al. 2017a).

229    All other clock rates were set on estimate. For 16S rRNA and EF1-alpha also relaxed log-normal

230    clock was used, whereas for 28S rRNA and ITS1 the strict clock was used. All the models were

231    tested beforehand in MEGA software, using implemented test for molecular clock model based

232    on Maximum Likelihood phylogeny (Kumar et al. 2016). The resulting trees were checked for

233    ESS values in Tracer and two trees with the best ESS values were combined in LogCombiner

234    and annotated in TreeAnnotator. The final output tree was edited in FigTree software

235    (http://tree.bio.ed.ac.uk/software/figtree/).

236    **Results**

237    ***Systematics***

238    Order: Amphipoda Latreille, 1818

239    Family: Gammaridae Leach, 1814

240    Genus: *Gammarus* Fabricius, 1775

241    Pinkster, 1970: 179, Karaman & Pinkster, 1977a: 3, Barnard & Barnard, 1983: 463.

242    Type species: *Cancer pulex* Linnaeus, 1758 [=*Gammarus pulex* (Linnaeus)] by subsequent

243    designation of Pinkster, 1970: 177 (neotype designation).

244    *Gammarus plaitisi* sp. nov

245    (Figs 2-6)

246    *Gammarus pulex pulex* (part.) Karaman, 2003: 31 (Vrondisi monastery, village Zaros, Creta

247    Island, Greece)

248    Diagnosis: Large species, making a robust impression. Similiar to *G. pulex pulex* by the

249    characteristic antenna 2 with swollen flagellum, bearing a flag-like dense brush of setae and

250    similar armature of pereiopods. It may be distinguished from *G. pulex pulex* by the lack of spines

251    on the dorsal surface of the first segment of urosome, the shape of the posterodistal margin of the

252    second and third epimeral plate and by the size and the arrangement of the pores on the cuticle

253    surface. It is also clearly distinguishable from *G. pulex pulex* on the molecular level, with respect

254    to the COI nucleotide sequence.

255    Materials examined: More than 200 individuals, both males and females, from 7 localities in

256    different parts of Crete Island, Greece: *small spring and stream at the Sfinari beach* N35.41533,

257    E23.56127, many individuals coll. 28 August 2011; *small stream in forest near Elos*, N35.36567,

258    E23.63718, many individuals coll. 28 August 2011; *Pelekaniotikos river near Kalamios*

259   N35.30729, E23.63583 many individuals coll. 28 August 2011; *stream near Viatos* N35.39724,

260   E23.65512, many individuals coll. 28 August 2011; *Pantomantris River in Fodele* N35.37828,

261   E24.95833, many individuals coll. 11 October 2015; *Springs in Astritsi* N35.19084, E25.22233,

262   many individuals coll. 9 October 2015; *Karteros River near Skalani* N35.28893, E25.20423,

263   many individuals coll. 9 October 2015.

264   Type: Holotype: An adult male individual collected on 11 October 2015, body length of 10 mm,

265   as well as the DNA voucher (extracted DNA in buffer) deposited in Museum and Institute of

266   Zoology Polish Academy of Sciences. Catalogue number: (MIZ 1/2018/1)); GenBank accession

267   number: (MG784515). Paratypes deposited in Museum and Institute of Zoology Polish Academy

268   of Sciences (catalogue numbers: MIZ 1/2018/2, MIZ 1/2018/3, MIZ 1/2018/4, MIZ 1/2018/5,

269   MIZ 1/2018/6) and Museum für Naturkunde in Berlin (catalogue number: ZMB 30868): five

270   specimens each fixed in 96% ethanol, collected from the type locality on 11 October 2015

271   Type locality: Crete Island, Pantomantris River in Fodele, Greece. N35.37828, E24.95833

272   Distribution and habitat: The species is endemic to Crete. It is found in freshwaters throughout

273   the island, usually in gravel, decomposing leaves and among submerged tree roots.

274   Etymology: This new species is named to honour the Cretan family Plaitis; particularly Wanda

275   and Manolis Plaitis from Fodele village, who hosted us and provided invaluable help during our

276   sampling expeditions to Crete.

277   Description: Male: Medium large, robust species with length up to 14 mm. *Head*: lateral lobes

278   rounded; eyes small; less than twice as long as wide. *Antenna I* (Fig. 2A): about half of the body

279   length, peduncle segments subsequently shorter with third segment about half length of the first

280   one. Main flagellum with 25–30 segments and accessory flagellum with 3-4 segments. Both

281   peduncle and flagellum with few short simple setae, rarely exceeding the diameter of segments.

282   *Antenna II* (Figs. 2B, 4B): Always shorter than antenna I. Peduncle segments armed with tufts of

283   short setae. Flagellum with 13 to 17 segments, which are swollen and compressed in adult

284   individuals; most segments armed with transverse rows of setae on the inner surface, altogether

285   forming a flag-like brush. Calceoli always present. *Mandibular palp* (Fig. 2C): First segment

286   unarmed. Second segment with ventral setae: in the proximal part 2–3 setae much shorter than

287   the diameter of the segment, in the distal part 10-13 setae as long as or up to 2.5× longer than the

288    diameter of the segment. Third segment armed with 2 groups of long A-setae, a regular comb of

289    25–30 D-setae and 5–6 long E-setae. *Maxillipeds* (Fig. 2D): The maxillipeds with the inner plate

290    armed distally with strong spine-teeth; the outer plate with spine-teeth and long plumose setae;

291    the palp is well developed. *Gnathopod I* (Fig. 2E): Palm oblique, setose, with one strong medial

292    palmar spine, strong angle spine accompanied by several small spines intermixed with longer

293    setae along the posterior palmar margin with addition of small spines and short setae on the

294    lateral surface. *Gnathopod II* (Fig. 2F): Propodus trapezoid, widening distally. Palm concave,

295    setose, with one medial palmar spine and three angle spines. Many groups of setae, variable in

296    length, are visible both on the inner and outer as well as the lateral surface of the propodus

297    *Pereopod III* (Fig. 3A): Anterior and distal margin of coxal plate slightly convex, posterior

298    margin straight. Distal corners rounded. The last three segments of third pereiopod bear groups

299    of long, often curved setae along the posterior margin, usualIy 2 to 3 times longer than the

300    diameter of segments. The anterior margin of merus armed with 1 spine. Dactylus short, robust

301    with one seta at joint of unguis. *Pereopod IV* (Fig. 3B): Coxal plate dilated distally. Distal

302    corners rounded. The last three segments of fourth pereiopod bear groups of long, often curved

303    setae along the posterior margin, usualIy 2 to 3 times longer than the diameter of segments. The

304    anterior margin of merus armed with 1 spine. Dactylus short, robust with one seta at joint of

305    unguis. *Pereopod V* (Fig. 3C): Basis with a subrectangular shape, posterior margin slightly

306    concave, posterodistal lobe well developed, posterior margin with 10-12 very short setae,

307    anterior margin with 4-5 spiniform setae. Ischium naked. Merus, carpus and propodus with

308    robust spines on both margins, occasionally intermixed with relatively short setae. Dactylus

309    short, robust usually with one seta at joint of unguis. *Pereopod VI* (Fig. 3D): Similar to PV, but

310    slightly longer and wider, posterior margin convex, posterodistal lobe less prominent and basis

311    more more elongated with a single, little spine on posterointerior corner. Ischium to propodus

312    armed with robust spines and very few short setae. Dactylus short, robust with one seta at joint of

313    unguis. *Pereopod VII* (Fig. 3E): Basis wider than in PVI with a single, little spine only at

314    posteroinferior corner and even more elongated. Further articles armed same as in preceding

315    pereopods. *Uropod III* (Fig. 3F): The inner ramus attains about 2/3 of the length of the outer

316    ramus. Most of setae along the inner and outer margin of endo- and exopodite plumose. *Telson*

317    (Fig. 3G): Deeply cleft, rather setose. Each lobe with 2 apical strong spines intermixed with few

318    short and long setae, several short subapical setae present. *Epimeral plates* (Fig. 3H): First

319    epimeral plate with 1 spine at the laterodistal margin. Second epimeral plate with 1 spine at the

320    laterodistal surface, posterodistal margin rounded. Third epimeral plate with 3 spines at the

321    laterodistal surface, posterodistal margin rounded with the posterodistal corner slightly pointed.

322    *Urosome* (Fig. 4A): very flat without any elevation. First urosomite lacking any spines on

323    dorsomedial or dorsolateral surface and armed only with a few groups of setae. Second

324    urosomite with dorsomedial and dorsolateral groups of robust spines (2–2–2). Third urosomite

325    only with two groups of dorsolateral spines on each side (3–0–3), and a dorsmedial group of 2-4

326    setae. *Ultrastructure* (Figs. 5, 6) The pores are larger and more distinctly marked in comparison

327    to *G. pulex pulex*. This pattern holds true for both A1 and E2, however on A1 the difference is

328    more pronounced. On A1 pores form the regular rows for both *G. plaitisi* sp.nov. and *G. pulex*

329    *pulex*, whereas on E2 the rows of pores are much more regular in *G. plaitisi* sp.nov. compared to

330    those in  *G. pulex pulex*. The distances between rows of pores are always about 1.5 times wider

331    than in *G. pulex pulex*. Female: Smaller than male. The setation of the peduncle segments of the

332    first and second antennae is longer than in the male. The characteristic brush of second antenna

333    flagellum is absent. The propodi of the gnathopods smaller than in males and the setation of P3

334    and P4 is less abundant and shorter.

335    Variability: Morphology of *G. plaiti* is stable with respect to features such as presence of calceoli

336    in males, presence of brush in peduncle of A2, flatness and armature of urosomites. Larger

337    individuals tend to have higher number of flagellum segments in antenna I and II, as well as

338    more and longer setae on all appendages. The density of the setation and spinulation is also

339    rather variable depending on age of the individual. Such variability is typical for most species of

340    this genus (Karaman and Pinkster 1977 a,b, 1987).

341    ***Haplotype diversity and phylogeny reconstruction***

342    We identified three haplotypes of *G. plaitisi* sp.nov. in the dataset composed of the forty three

343    COI sequences, with one haplotype being represented only by one specimen. The most common

344    haplotype, H2, was present in the majority of sites, except for locus typicus of the species (Fig.

345    7). The overall haplotype diversity was quite high (Hd= 0,375 ± 0,076), whereas nucleotide

346    diversity (Pi= 0,00126 ± 0,00075) was low. Generally, the differentiation was very low as the

347    most common haplotype differed from the two remaining ones by a maximum of two mutation

348    steps with intraspecific distance not exceeding the value of 0.005.

349    All MOTU delimitation methods supported distinctness of *G. plaitisi*, which always formed a

350    single MOTU and was separated from its closest relative by the mean K2P distance of 0.12 (Tab.

351    S1). It also formed a unique BIN in the BOLD database (BOLD: ADG8205). All the applied

352    MOTU delimitation methods provided constant results with six MOTUs delimited for the *G.*

353    *pulex* morphospecies. Only the ABGD method indicated one MOTU less within the Peloponnese

354    group. Both the used GMYC approaches produced the same outcome with the same LR test

355    values. Results of MOTU delimitation methods support high cryptic diversity within *Gammarus*

356    *pulex* morphospecies from Greece, as no morphological differences amongst the representatives

357    of respective MOTUs have been found. The topology of the neighbour-joining tree confirms that

358    *G. plaitisi* sp. nov. is nested within the clade of lineages belonging to the *G. pulex* morphospecies

359    (Fig. 8). This suggests that *G. pulex* is, in reality, a paraphyletic group of cryptic and

360    pseudocryptic species.

361    Multimarker time-calibrated phylogeny indicated that divergence of the whole *G. pulex* lineages

362    from Peloponnese happened around 15 million years ago, whereas divergence of *G. plaitisi*

363    sp.nov. from its continental relatives took place around 9.2 million years ago  Moreover,

364    divergence within the continental groups of *G. pulex* lineages spanned the last 5 million years

365    (Fig.9). All three rates used for time calibratead reconstruction of Bayesian phylogeny gave

366    congruent results (Tab.2).

367    **Discussion**

368    We provided evidence for the existence of new freshwater *Gammarus* species from Crete,

369    making this the third known freshwater endemic gammarid to Crete. The endemic freshwater

370    species of Gammaridae before this work were, *Echinogammarus platvoeti* and *E. kretensis*

371    (Pinkster 1993), making *G. plaitisi* sp. nov. the first endemic of the genus *Gammarus*. The

372    integrative taxonomy approach confirmed the distinctness of the species not only on a

373    morphological basis, but also on a molecular level. This study also stressed the importance of

374    using SEM photography, which may provide additional diagnostic features that are impossible to

375    detect on usually used optical devices (Platvoet et al. 2008).

376    Despite the presence of *G. plaitisi* sp. nov. in seven, mostly isolated sites located both in the

377    eastern and western part of Crete, its haplotype diversity is surprisingly low, with only two

378    mutation steps separating the three known haplotypes (Tab. 3). This pattern suggests a strong

379    founder effect and recent dispersal, probably in the late Pleistocene, as suggested by the time-
380    calibrated phylogeny, possibly due to rearrangement of the local hydrological networks at the
381    end of the last Ice Age. This is a rather unusual finding considering the fact that Pleistocene
382    glaciations, which strongly affected the river systems, promoted the diversification of various
383    taxa in the Mediterranean (Previšić et al. 2009, Goncalves et al. 2015), including the freshwater
384    gammarids (Grabowski et al. 2017a). However, such a founder effect scenario has also been
385    found in other freshwater members of the genus *Gammarus*, such as *Gammarus minus* which
386    inhabits both surface and groundwaters of North America. Gooch and Glazier (1986) confirmed
387    postglacial dispersal of this species from refugia, which resulted in strong decrease in their allele
388    diversity. This scenario is the most plausible one also for *G. plaitisi* sp. nov., which may have
389    colonised the current distribution area from a single refugium. The distribution of haplotypes
390    (Fig. 7) suggests that the individuals originate from a founding population from the western part
391    of Crete, where all of the known haplotypes are present. Yet another question concerns the way
392    of dispersal between isolated freshwater systems, separated by more than 100 km. One must
393    consider passive dispersal i.e. by birds (Rachalewski et al. 2013), however, groundwater
394    connections cannot be excluded (Harris et al. 2002). On the other side, there may be still some
395    localities, particularly in the mountains, where the species is present or could have been present
396    in the early Holocene but died out due to climatic changes. We still do not have enough data to
397    reveal the dispersal history of this species.

398    Our results suggest that *G. plaitisi* sp. nov. has diverged from the continental lineages of *G. pulex*
399    around 9 million years ago (Fig. 9). This result has been strongly supported by cross-validation
400    with other substitution rates proposed for freshwater gammarids in earlier studies (Grabowski et
401    al. 2017a). The timescale seems to be convergent with the estimated date of the first isolation of
402    Crete from Peloponnese (Poulakakis et al. 2015). Since that time Crete could be colonized only
403    by overseas dispersal. This finding suggests the continental origin of the newly described
404    species. The molecular data suggest rather the possibility of its dispersal to Crete before first
405    isolation of this island than migration during the temporal land connection during the Messinian
406    Sality Crysis and after its final isolation at around 5 million years ago.

407    The closest known relatives to *G. plaitisi* sp.nov. are continental lineages of *G. pulex* from
408    Peloponnese and the northern Greece (Fig. 8). These continental lineages diverged from each

409    other around 5 million years ago, during the time of the Messinian Salinity Crisis (5.96-5.33

410    Mya), when the Mediterranean Basin dessicated (Krijgsman et al. 1999). The reopening of the

411    Strait of Gibraltar ended the Messinian Salinity Crisis and resulted in refilling of the basin (Hsu

412    et al. 1977). Nesting of *G. plaitisi* sp. nov. in between lineages of *G. pulex pulex* confirms the

413    already known lack of monophyly present in a number of freshwater gammarid morphospecies

414    (i.e. Hou et al. 2011, 2014, Weiss et al. 2014, Mamos et al. 2014, 2016; Copilaş-Ciocianu and

415    Petrusek 2015, 2017; Katouzian et al. 2016, Grabowski et al. 2017a,b). These data support the

416    need for a comprehensive revision of *Gammarus pulex*.

417    **Conclusions**

418    *G. plaitisi* sp. nov. is the first endemic insular freshwater *Gammarus* in the Mediterranean.

419    However, given the scarcity of the sampling in the fresh waters of the Mediterranean islands,

420    there is a high chance there are more representatives of the genus in the Aegean Basin and other

421    Mediterranean islands. The description of this new species using the integrative taxonomy

422    approach not only broadens the knowledge about freshwater diversity of Crete, but also provides

423    a link between the geological history of this island with the evolution of the local freshwater

424    species. The results provide yet another piece of the puzzle in explaining the evolution of the

425    family Gammaridae.

426    **Acknowledgments**

427    The first author would like to thank Charles Oliver Coleman for extremely valuable digital

428    drawing training. Mrs Marla Spencer from University of Southampton, UK, kindly agreed to

429    perform language corrections. We also thank the colleagues involved in sampling expeditions to

430    Crete: Karolina Bącela-Spychalska, Tomasz Rewicz, Piotr Gadawski, Aleksandra Bańkowska,

431    Andrzej Zawal, Agnieszka Szlauer-Łukaszewska.

432    **References:**

433    Alther, R., Fišer, C., & Altermatt, F. 2016. Description of a widely distributed but overlooked
434    amphipod species in the European Alps. Zoological Journal of the Linnean Society, 179(4), 751-
435    766.

436    Altschul, S.F., Gish, W., Miller, W., Myers, E.W., & Lipman, D.J. 1990. Basic local alignment
437    search tool. Journal of molecular biology, 215(3), 403-410.

438 Astrin, J.J., Stüben, P.E. 2011. Molecular phylogeny of Echinodera and Ruteria (Coleoptera:
439 Curculionidae: Cryptorhynchinae) and the parallel speciation of Canary Island weevils along
440 replicate environmental gradients. Invertebrate Systematics, 24(5), 434-455.

441 Bandelt, H., Forster, P., Röhl, A. 1999. Median-joining networks for inferring intraspecific
442 phylogenies. Molecular Biology and Evolution 16(1), 37-48.

443 Barnard, J.L., Barnard, C.M. 1983. Freshwater Amphipoda of the World: Handbook and
444 bibliography. Hayfield Associates.

445 Bilton, D.T., Freeland, J.R., Okamura, B. 2001. Dispersal in freshwater invertebrates. Annual
446 review of ecology and systematics, 159-181.

447 Bouckaert, R., Heled, J., Kühnert, D., Vaughan, T., Wu, C.H., Xie, D., ... & Drummond, A.J.
448 2014. BEAST 2: a software platform for Bayesian evolutionary analysis. PLoS computational
449 biology, 10(4), e1003537.

450 Bouckaert, R.R., Drummond, A.J. 2017. bModelTest: Bayesian phylogenetic site model
451 averaging and model comparison. BMC evolutionary biology, 17(1), 42.

452 Brower, A.V. 1994. Rapid morphological radiation and convergence among races of the butterfly
453 Heliconius erato inferred from patterns of mitochondrial DNA evolution. Proceedings of the
454 National Academy of Sciences, 91(14), 6491-6495.

455 Chu, K.H., Li, C.P., Ho, H.Y. 2001. The first internal transcribed spacer (ITS-1) of ribosomal
456 DNA as a molecular marker for phylogenetic and population analyses in Crustacea. Marine
457 Biotechnology, 3(4), 355-361.

458 Coleman, C.O. 2006. Substituting time-consuming pencil drawings in arthropod taxonomy using
459 stacks of digital photographs. Zootaxa, 1360(1), 61-68.

460 Coleman, C.O. 2009. Drawing setae the digital way. Zoosystematics and Evolution, 85(2), 305-
461 310.

462 Copilaş-Ciocianu D, Petrusek A 2015. The southwestern Carpathians as an ancient centre of
463 diversity of freshwater gammarid amphipods: insights from the *Gammarus fossarum* species
464 complex. *Molecular ecology* 24(15): 3980-3992

465 Copilaş-Ciocianu, D., Petrusek, A. 2017. Phylogeography of a freshwater crustacean species
466 complex reflects a long-gone archipelago. *Journal of Biogeography* 44(2): 421-432

467 Costa, F.O., DeWaard, J.R., Boutillier, J., Ratnasingham, S., Dooh, R.T., Hajibabaei, M., Hebert,
468 P.D. 2007. Biological identifications through DNA barcodes: the case of the Crustacea. Canadian
469 Journal of Fisheries and Aquatic Sciences, 64(2), 272-295.

470 Fabricius, J.C. 1775. Systema Entomologiae, sistens Insectorum Classes, Ordines, Genera,
471 Species, adjectis synonymus, locis, descriptionibus, obserbationibus. in Flensburgi et Lipsiae:
472 832 pp.

473 Figueroa, J.M.T., López-Rodríguez, M.J., Fenoglio, S., Sánchez-Castillo, P., Fochetti, R. 2013.
474 Freshwater biodiversity in the rivers of the Mediterranean Basin. Hydrobiologia, 719(1), 137-
475 186.

476 Folmer, O., Black, M., Hoeh, W., Lutz, R., Vrijenhoek, R. 1994. DNA primers for amplification
477 of mitochondrial cytochrome c oxidase subunit I from diverse metazoan invertebrates. Molecular
478 Marine Biology and Biotechnology, 3, 294–299.

479 Gooch, J.L., Glazier, D.S. 1986. Levels of heterozygosity in the amphipod *Gammarus minus* in
480 an area affected by Pleistocene glaciation. American Midland Naturalist, 57-63.

481 Goncalves, H., Maia-Carvalho, B., Sousa-Neves, T., Garcia-Paris, M., Sequeira, F., Ferrand,
482 Martinez-Solano, N.I. 2015. Multi locus phylogeography of the common midwife toad, *Alytes*
483 *obstetricans* (Anura, Alytidae): contrasting patterns of lineage diversification and genetic
484 structure in the Iberian refugium. Molecular Phylogenetics and Evolution 93:363–379

485 Grabner, D. S., Weigand, A. M., Leese, F., Winking, C., Hering, D., Tollrian, R., & Sures, B.
486 2015. Invaders, natives and their enemies: distribution patterns of amphipods and their
487 microsporidian parasites in the Ruhr Metropolis, Germany. Parasites & vectors, 8(1), 419.

488 Grabowski, M., Mamos, T., Bącela-Spychalska, K., Rewicz, T., Wattier, R.A. 2017a. Neogene
489 paleogeography provides context for understanding the origin and spatial distribution of cryptic
490 diversity in a widespread Balkan freshwater amphipod. *PeerJ* 5: e3016

491 Grabowski, M., Wysocka, A., Mamos, T. 2017b. Molecular species delimitation methods
492 provide new insight into taxonomy of the endemic gammarid species flock from the ancient Lake
493 Ohrid. Zoological Journal of the Linnean Society, zlw025.

494 Harris, P.M., Roosa, B.R., Norment, L. 2002. Underground dispersal by amphipods (*Crangonyx*
495 *pseudogracilis*) between temporary ponds. Journal of Freshwater Ecology, 17(4), 589-594.

496 Hebert, P.D., Cywinska, A., Ball, S.L. 2003. Biological identifications through DNA barcodes.
497 Proceedings of the Royal Society of London B: Biological Sciences, 270(1512), 313-321.

498 Hillis, D.M., Moritz, C., Mable, B.K.. 1996. Molecular systematics. Sinauer Associates.
499 Sunderland, MA, USA.

500 Hou, Z., Fu, J., Li, S. 2007. A molecular phylogeny of the genus *Gammarus* (Crustacea:
501 Amphipoda) based on mitochondrial and nuclear gene sequences. *Molecular Phylogenetics and*
502 *Evolution* 45(2): 596-611

503 Hou, Z., Sket, B., Fišer, C., Li, S. 2011. Eocene habitat shift from saline to freshwater promoted
504 Tethyan amphipod diversification. Proceedings of the National Academy of Sciences, 108(35),
505 14533-14538.

506 Hou, Z., Sket, B., Li, S. 2014. Phylogenetic analyses of Gammaridae crustacean reveal different
507 diversification patterns among sister lineages in the Tethyan region. Cladistics, 30(4), 352-365.

508 Hsü, K.J., Montadert, L., Bernoulli, D., Cita, M.B., Erickson, A., Garrison, R.E., ... & Wright, R.
509 1977. History of the Mediterranean salinity crisis. Nature, 267(5610), 399-403.

510 Karaman, G.S. 2003. New data on some gammaridean amphipods (Amphipoda, Gammaridea)
511 from Palearctic. Glasnik of the Section of Natural Sciences Montenegrin Academy of Sciences
512 and Arts, 15, 20-37.

513   Karaman, G.S., Pinkster, S., 1977a. Freshwater *Gammarus* species from Europe, North Africa
514   and adjacent regions of Asia (Crustacea, Amphipoda). Part I. *Gammarus pulex*-group and related
515   species. Bijdr. Dierk. 47, 1–97.

516   Karaman, G.S., Pinkster, S., 1977b. Freshwater *Gammarus* species from Europe, North Africa
517   and adjacent regions of Asia (Crustacea,Amphipoda).PartII. *Gammarus roeseli*-group and related
518   species. Bijdr. Dierk. 47, 165–196.

519   Karaman, G.S., Pinkster, S., 1987. Freshwater *Gammarus* species from Europe, North Africa and
520   adjacent regions of Asia (Crustacea,Amphipoda).Part III. *Gammarus balcanicus*-group and
521   related species. Bijdr. Dierk. 57, 207–260.

522   Katoh, K., Misawa, K., Kuma, K. I., Miyata, T. 2002. MAFFT: a novel method for rapid
523   multiple sequence alignment based on fast Fourier transform. Nucleic acids research, 30(14),
524   3059-3066.

525   Katouzian, A.R., Sari, A., Macher, J.N., Weiss, M., Saboori, A., Leese, F., Weigand, A.M. 2016.
526   Drastic underestimation of amphipod biodiversity in the endangered Irano-Anatolian and
527   Caucasus biodiversity hotspots. *Scientific reports* 6

528   Kearse, M., Moir, R., Wilson, A., Stones-Havas, S., Cheung, M., Sturrock, S., ... & Thierer, T.
529   2012. Geneious Basic: an integrated and extendable desktop software platform for the
530   organization and analysis of sequence data. Bioinformatics, 28(12), 1647-1649.

531   Kelly, D.W., Dick, J.T., Montgomery, W.I. 2002. The functional role of *Gammarus* (Crustacea,
532   Amphipoda): shredders, predators, or both?. Hydrobiologia, 485(1-3), 199-203.

533   Krijgsman, W., Hilgen, F.J., Raffi, I., Sierro, F.J., Wilson, D.S. 1999. Chronology, causes and
534   progression of the Messinian salinity crisis. Nature, 400(6745), 652-655.

535   Kumar, S., Stecher, G., Tamura, K. 2016. MEGA7: Molecular Evolutionary Genetics Analysis
536   version 7.0 for bigger datasets. Molecular biology and evolution, 33(7), 1870-1874.

537   Kunz, P.Y., Kienle, C., Gerhardt, A. 2010. *Gammarus* spp. in aquatic ecotoxicology and water
538   quality assessment: toward integrated multilevel tests. In Reviews of Environmental
539   Contamination and Toxicology Volume 205 (pp. 1-76). Springer New York.

540   Latreille, P.A. 1818. Crustaces, arachnides et insectes. Tableau Encyclopedique et Methodique
541   des Trois Regnes de la Nature. Paris 24(6): 142 pp.

542   Leach, W.E. 1814. Crustaceology. The Edinburgh Encyclopaedia 7:402-435.

543   Leigh, J.W., Bryant, D. 2015. PopART: full-feature software for haplotype network construction.
544   *Methods in Ecology and Evolution* 6(9): 1110-1116

545   Librado, P., Rozas, J. 2009. DnaSP v5: a software for comprehensive analysis of DNA
546   polymorphism data. *Bioinformatics* 25(11): 1451-1452

547   Linnaeus, C. 1758. Systema Naturae, Editio Decima, Tomus I. Holmiae [Stockholm]: Laurenti
548   Salvii.

549   MacDonald III, K. S., L. Yampolsky & J. Duffy, 2005. Molecular and morphological evolution
550   of the amphipod radiation of Lake Baikal. Molecular Phylogenetics and Evolution 35: 323–343.

551 MacNeil, C., Dick, J. T., & Elwood, R. W. 1997. The trophic ecology of freshwater Gammarus
552 spp.(Crustacea: Amphipoda): problems and perspectives concerning the functional feeding group
553 concept. Biological Reviews of the Cambridge Philosophical Society, 72(03), 349-364.

554 Mamos, T., Wattier, R., Majda, A., Sket, B., Grabowski, M. 2014. Morphological vs. molecular
555 delineation of taxa across montane regions in Europe: the case study of *Gammarus balcanicus*
556 Schäferna (Crustacea: Amphipoda). *Journal of Zoological Systematics and Evolutionary*
557 *Research* 52(3): 237-248

558 Mamos, T., Wattier, R., Burzyński, A., Grabowski, M. 2016. The legacy of a vanished sea: a
559 high level of diversification within a European freshwater amphipod species complex driven by
560 15 My of Paratethys regression. *Molecular ecology* 25(3): 795-810

561 Monaghan, M.T., Wild, R., Elliot, M., Fujisawa, T., Balke, M., Inward, D.J., ... & Vogler, A. P.
562 2009. Accelerated species inventory on Madagascar using coalescent-based models of species
563 delineation. Systematic biology, 58(3), 298-311.

564 Myers, N., Mittermeier, R.A., Mittermeier, C.G., Da Fonseca, G.A., & Kent, J. 2000.
565 Biodiversity hotspots for conservation priorities. Nature, 403(6772), 853-858.

566 Neuparth, T., Costa, F.O., Costa, M.H. 2002. Effects of temperature and salinity on life history
567 of the marine amphipod *Gammarus locusta*. Implications for ecotoxicological testing.
568 Ecotoxicology, 11(1), 61-73.

569 Neuparth, T., Correia, A.D., Costa, F.O., Lima, G., Costa, M.H. 2005. Multi-level assessment of
570 chronic toxicity of estuarine sediments with the amphipod *Gammarus locusta*: I. Biochemical
571 endpoints. Marine environmental research, 60(1), 69-91.

572 Palumbi, S., Martin, A., Romano, S., Mcmillan, W., Stice L., Grabowski G. 1991. The Simple
573 Fool's Guide to PCR. A Collection of PCR Protocols, Version 2. University of Hawaii, Honolulu

574 Pinkster, S. 1970. Redescription of *Gammarus pulex* (Linnaeus, 1758) based on neotype material
575 (Amphipoda). Crustaceana, 18(2), 177-186.

576 Pinkster, S. 1993. A revision of the genus *Echinogammarus* Stebbing, 1899 with some notes on
577 related genera (Crustacea, Amphipoda). Memorie Del Museo Civico Di Storia Naturale, pp. 1–
578 185.

579 Platvoet, D., Hou, Z.E., Li, S., van der Velde, G. 2008. The Amphipod Pilot Species Project
580 (AMPIS), a novel Dutch-Chinese taxonomic initiative (Peracarida, Amphipoda): a description of
581 the project. Crustaceana, 81(8), 989-992.

582 Pons, J., Barraclough, T.G., Gomez-Zurita, J., Cardoso, A., Duran, D.P., Hazell, S., ... & Vogler,
583 A.P. 2006. Sequence-based species delimitation for the DNA taxonomy of undescribed insects.
584 Systematic biology, 55(4), 595-609.

585 Poulakakis, N., Kapli, P., Lymberakis, P., Trichas, A., Vardinoyiannis, K., Sfenthourakis, S.,
586 Mylonas, M. 2015. A review of phylogeographic analyses of animal taxa from the Aegean and
587 surrounding regions. Journal of Zoological Systematics and Evolutionary Research, 53(1), 18-32.

588   Previšić, A., Walton, C., Kučinić, M., Mitrikeski, P. T., Kerovec, M. 2009. Pleistocene
589   divergence of Dinaric Drusus endemics (Trichoptera, Limnephilidae) in multiple microrefugia
590   within the Balkan Peninsula. Molecular ecology, 18(4), 634-647.

591   Puillandre, N., Lambert, A., Brouillet, S., Achaz, G. 2012. ABGD, Automatic Barcode Gap
592   Discovery for primary species delimitation. Molecular ecology, 21(8), 1864-1877.

593   Rachalewski, M., Banha, F., Grabowski, M., Anastácio, P. M. 2013. Ectozoochory as a possible
594   vector enhancing the spread of an alien amphipod *Crangonyx pseudogracilis*. Hydrobiologia,
595   717(1), 109-117.

596   Ratnasingham, S., Hebert, P.D. 2007. BOLD: The Barcode of Life Data System (http://www.
597   barcodinglife. org). Molecular Ecology Resources, 7(3), 355-364.

598   Ratnasingham, S., Hebert, P.D. 2013. A DNA-based registry for all animal species: the Barcode
599   Index Number (BIN) system. PloS one, 8(7), e66213.

600   Seutin, G., White, B.N., Boag, P.T. 1991. Preservation of avian blood and tissue samples for
601   DNA analyses. Canadian Journal of Zoology, 69(1), 82-90.

602   Sondaar P.Y., Dermitzakis M.D. 1982. Relation Migration Landvertebrates, Paleogeography and
603   Tectonics. In: Pichon X.L., Augustidis S.S., MascleJ. (eds), International Symposium on the
604   Hellenic Arc and Trench (H.E.A.T.), April 8–10 1981, Athens, 2: 283–308.

605   Stebbing, T.R.R. 1899. Revision of Amphipoda. Annals and Magazine of Natural History, series
606   7, 4: 205-211.

607   Weiss, M., Macher, J.N., Seefeldt, M.A., Leese, F. 2014. Molecular evidence for further
608   overlooked species within the *Gammarus fossar*um complex (Crustacea: Amphipoda).
609   *Hydrobiologia* 721(1): 165

610   Whittaker, R.J., Fernández-Palacios, J.M. 2007. Island biogeography: ecology, evolution, and
611   conservation. Oxford University Press.

612   Woodward, J. (Ed.). 2009. The physical geography of the Mediterranean (Vol. 8). Oxford
613   University Press on Demand.

614   Wysocka, A., Grabowski, M., Sworobowicz, L., Mamos, T., Burzyński, A., Sell, J. 2014. Origin
615   of the Lake Ohrid gammarid species flock: ancient local phylogenetic lineage diversification.
616   Journal of Biogeography, 41(9), 1758-1768.

617   Zhang, J., Kapli, P., Pavlidis, P., Stamatakis, A. 2013. A general species delimitation method
618   with applications to phylogenetic placements. Bioinformatics, 29(22), 286.

619

620   Figure captions:

621   Fig.1 Map of the sampling sites on Crete. Purple dots indicate sites, that were visited where no

622   individuals of **Gammarus plaitisi** sp. nov. were found. Blue dots represent the sites where *G.*

623   *plaitisi* sp. nov. specimens were found.

624    Fig.2 *Gammarus plaitisi* sp. nov. male, paratype, 13 mm, locus typicus, Fodele, Crete. A:
625    antenna 1, outer face; B: antenna II, outer face; C: mandibular palp, inner face; D: maxillipeds,
626    outer face; E: palm of gnathopod I, outer face; F: palm of gnathopod II, outer face.

627    Fig.3 *Gammarus plaitisi* sp. nov. male, paratype, 13 mm, locus typicus, Fodele, Crete. A-B:,
628    pereopod III and IV, outer face; C-E: pereopod V to VII; F: uropod III; G: telson.

629    Fig.4 *Gammarus plaitisi* sp. nov. male, paratype, 12 mm, locus typicus, Fodele, Crete. A-B:
630    Epimeral plates II and III; C: urosome, dorsal view; D: calceola.

631    Fig.5 Comparison of the ultrastructure of a fragment of antenna I of *Gammarus plaitisi* sp. nov.,
632    Fodele, Crete; *Gammarus pulex pulex*, Estonia.

633    Fig.6 Comparison of the ultrastructure of a fragment of epimeral plate II of *Gammarus plaitisi*
634    sp. nov., Fodele, Crete; *Gammarus pulex pulex*, Estonia.

635    Fig.7 Map of the sampling sites on Crete with the median-joining haplotype network of
636    *Gammarus plaitisi* sp. nov.. Circles indicate the frequency of haplotypes at each particular site.

637    Fig.8 Neighbor-joining tree of the *Gammarus plaitisi* sp. nov. with members of *Gammarus* cf.
638    *pulex*, obtained from our data and mined from NCBI GenBank with the addition of the
639    outgroups. The numbers by respective nodes indicate bootstrap values ≥ 0.75. The scale bar
640    corresponds to the number of substitutions per site. The rows of respective bars represent the
641    delimitation of molecular operational taxonomic units (MOTU) by various methods of species
642    delimitation.

643    Fig.9 Maximum clade credibility, time-calibrated Bayesian reconstruction of phylogeny of the
644    *Gammarus plaitisi* sp. nov. with members of *Gammarus* cf. *pulex* from Peloponnese and
645    Northern Greece. Phylogeny was inferred from sequences of the mitochondrial COI and 16S
646    genes and nuclear 28S, ITS1 and EF1-α genes. The numbers by respective nodes indicate
647    Bayesian posterior probability values ≥ 0.85. Grey bars indicate the respective MOTUs of
648    *Gammarus* morphospecies and grey node bars represent 95% HPD.

# Figure 1

Map of the sampling sites on Crete.

Purple dots indicate sites, that were visited where no individuals of **Gammarus plaitisi** sp. nov. were found. Blue dots represent the sites where *G. plaitisi* sp. nov. specimens were found.
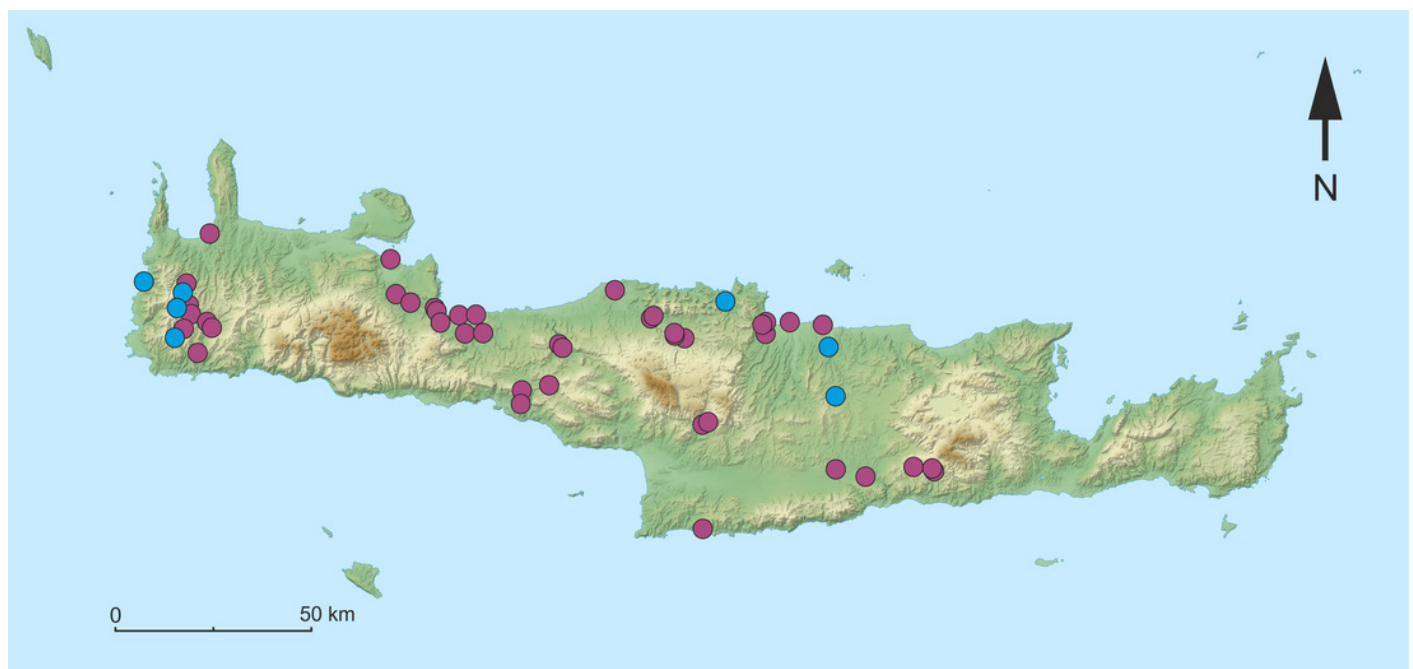
# Figure 2

*Gammarus plaitisi* sp. nov. male, paratype, 13 mm, locus typicus, Fodele, Crete.

A: antenna 1, outer face; B: antenna II, outer face; C: mandibular palp, inner face; D: maxillipeds, outer face; E: palm of gnathopod I, outer face; F: palm of gnathopod II, outer face

A

B

C

D

E

F
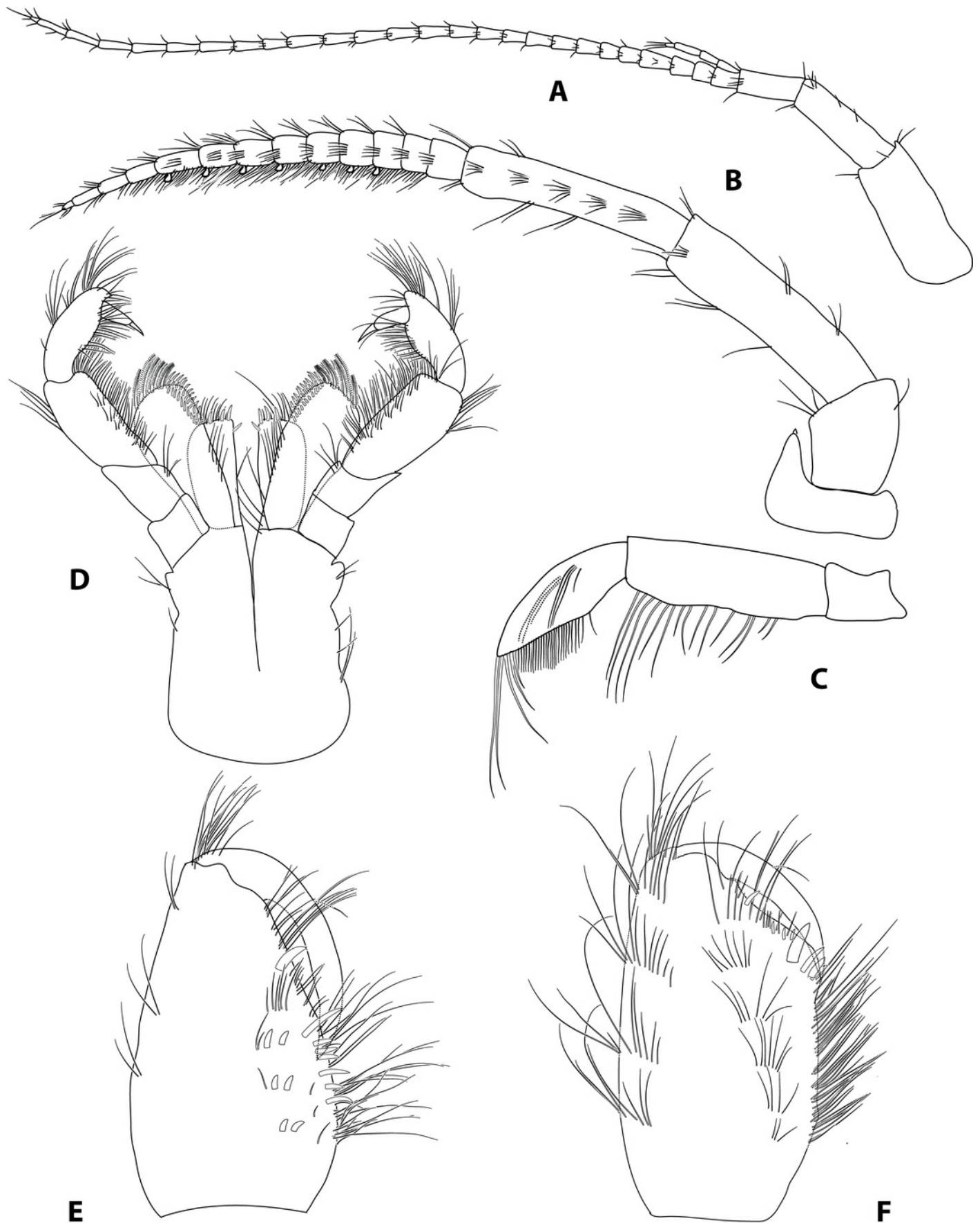
# Figure 3

*Gammarus plaitisi* sp. nov. male, paratype, 13 mm, locus typicus, Fodele, Crete.

A-B:, pereopod III and IV, outer face; C-E: pereopod V to VII; F: uropod III; G: telson.
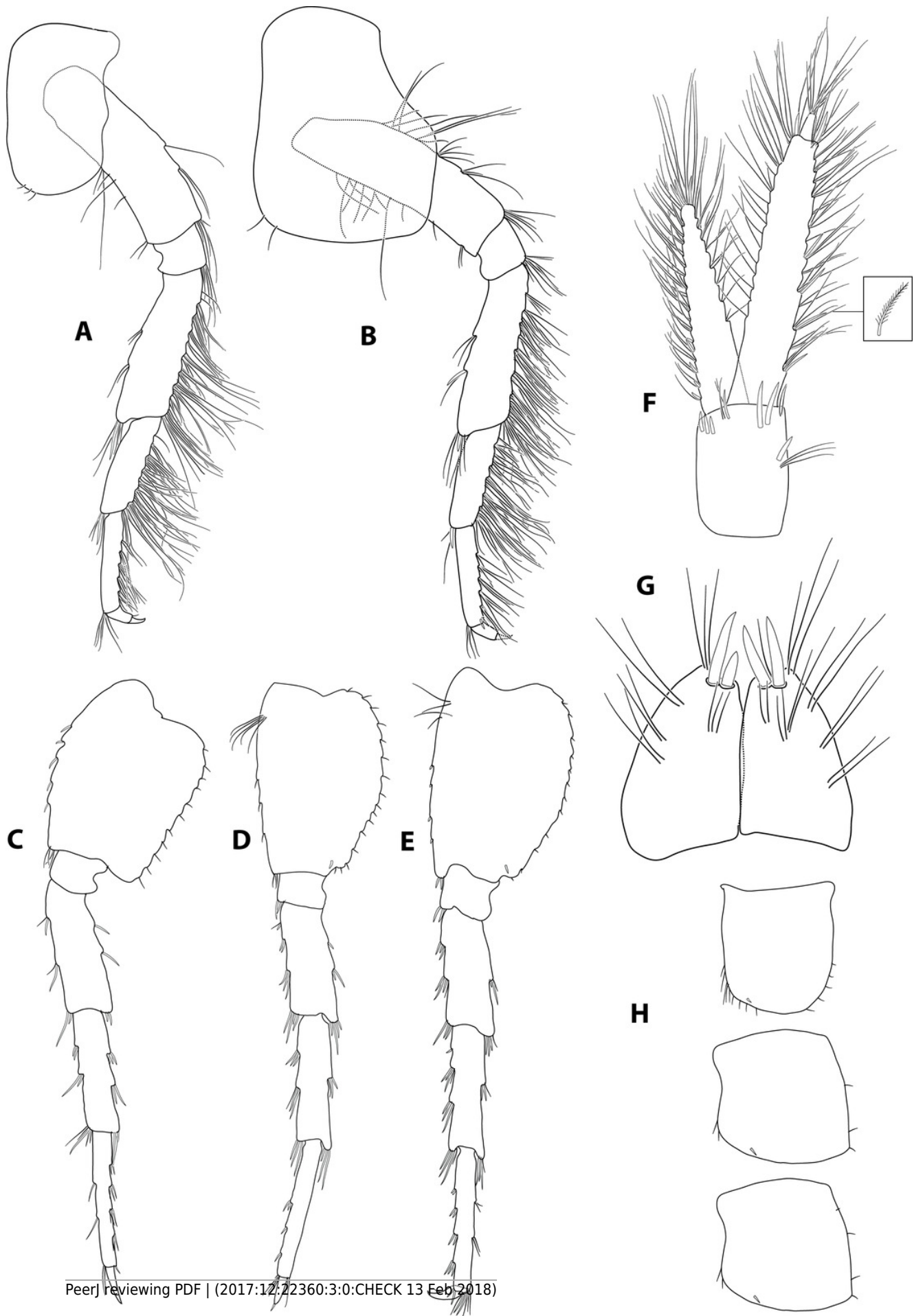
# Figure 4

*Gammarus plaitisi* sp. nov. male, paratype, 12 mm, locus typicus, Fodele.

Crete. A-B: Epimeral plates II and III; C: urosome, dorsal view; D: calceola.

*Note: Auto Gamma Correction was used for the image. This only affects the reviewing manuscript. See original source image if needed for review.*
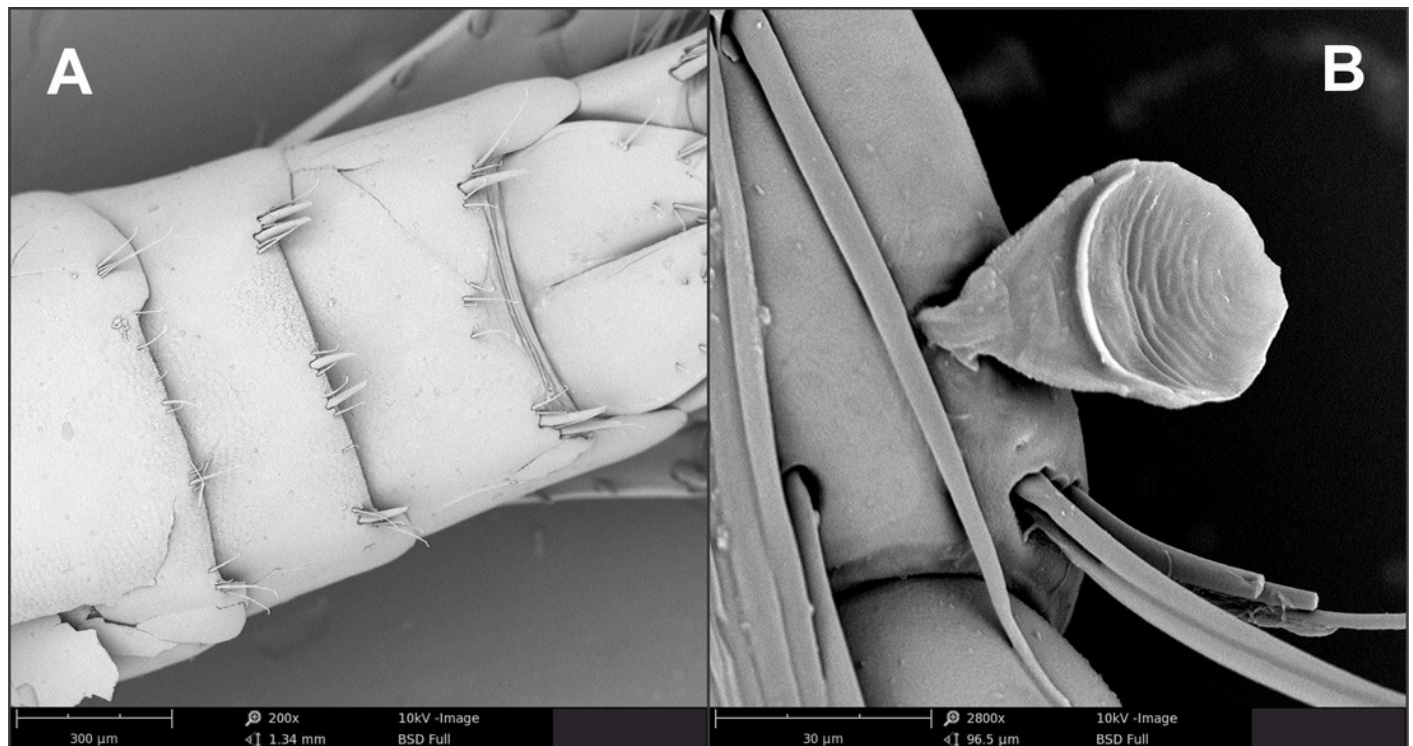
# Figure 5

Comparison of the ultrastructure of a fragment of antenna I of *Gammarus plaitisi* sp. nov., Fodele, Crete; *Gammarus pulex pulex*, Estonia.
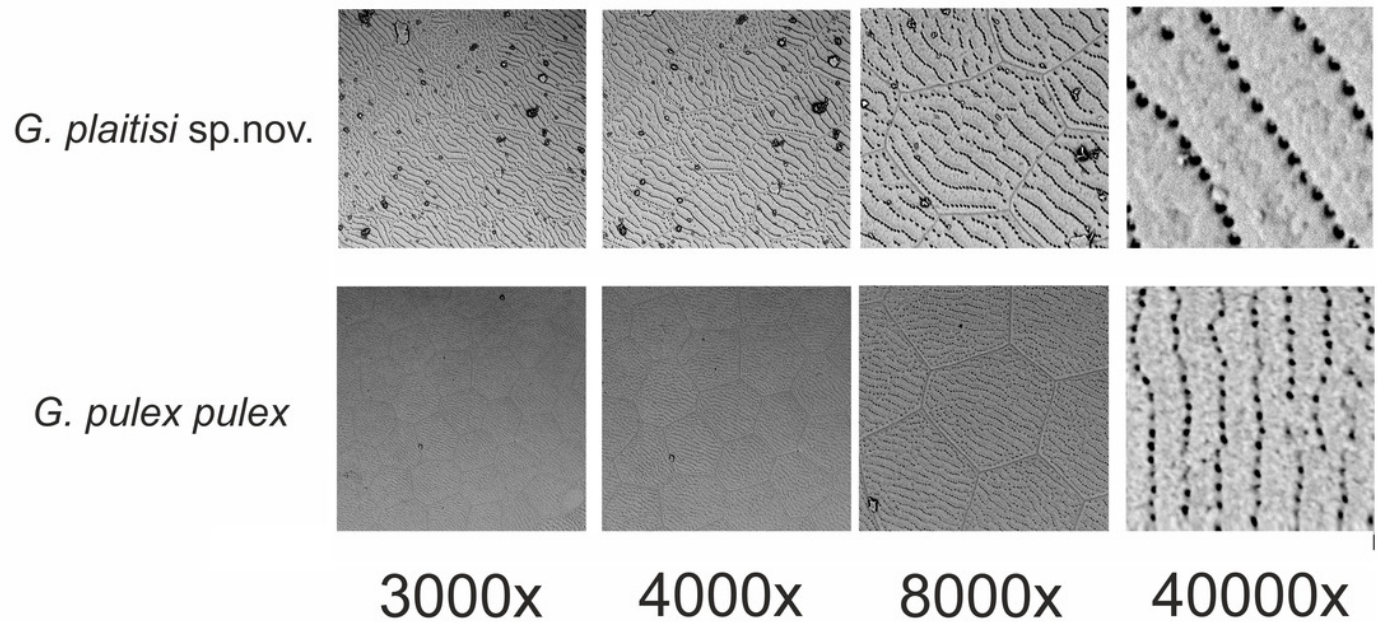
# Figure 6

Comparison of the ultrastructure of a fragment of epimeral plate II of *Gammarus plaitisi* sp. nov., Fodele, Crete; *Gammarus pulex pulex*, Estonia.
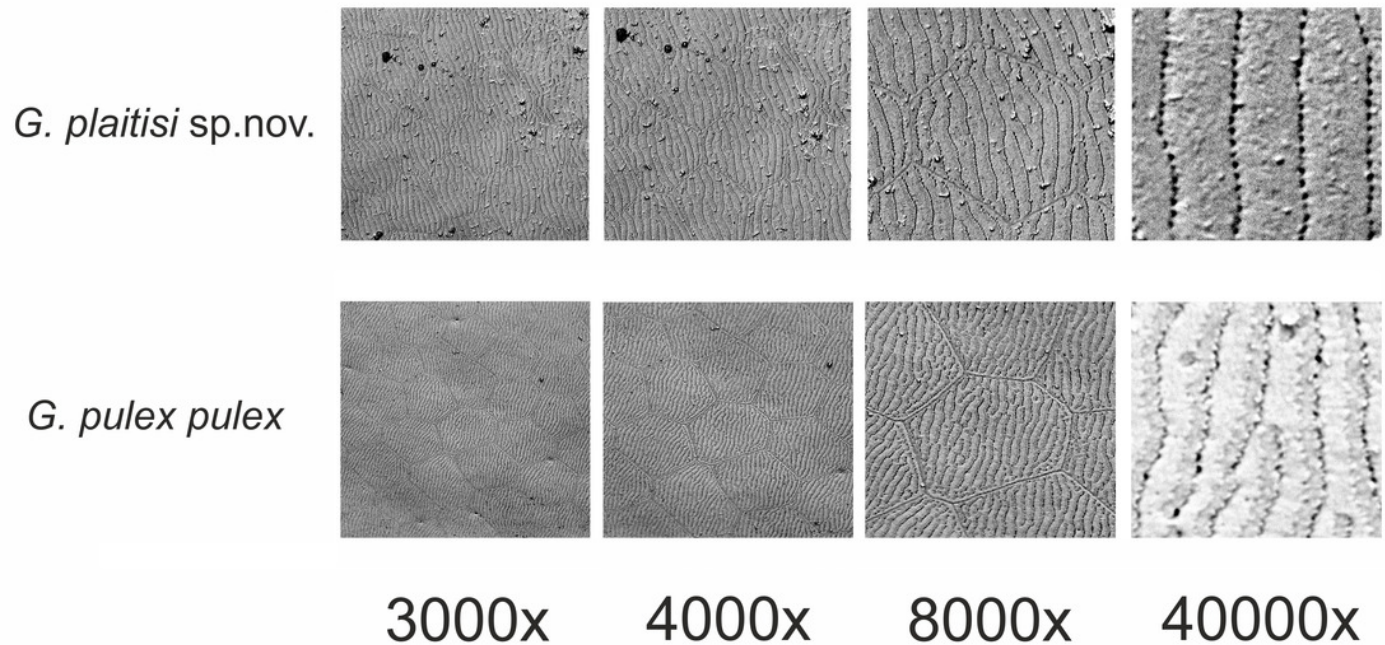
# Figure 7

Map of the sampling sites on Crete with the median-joining haplotype network of *Gammarus plaitisi* sp. nov..

Circles indicate the frequency of haplotypes at each particular site.
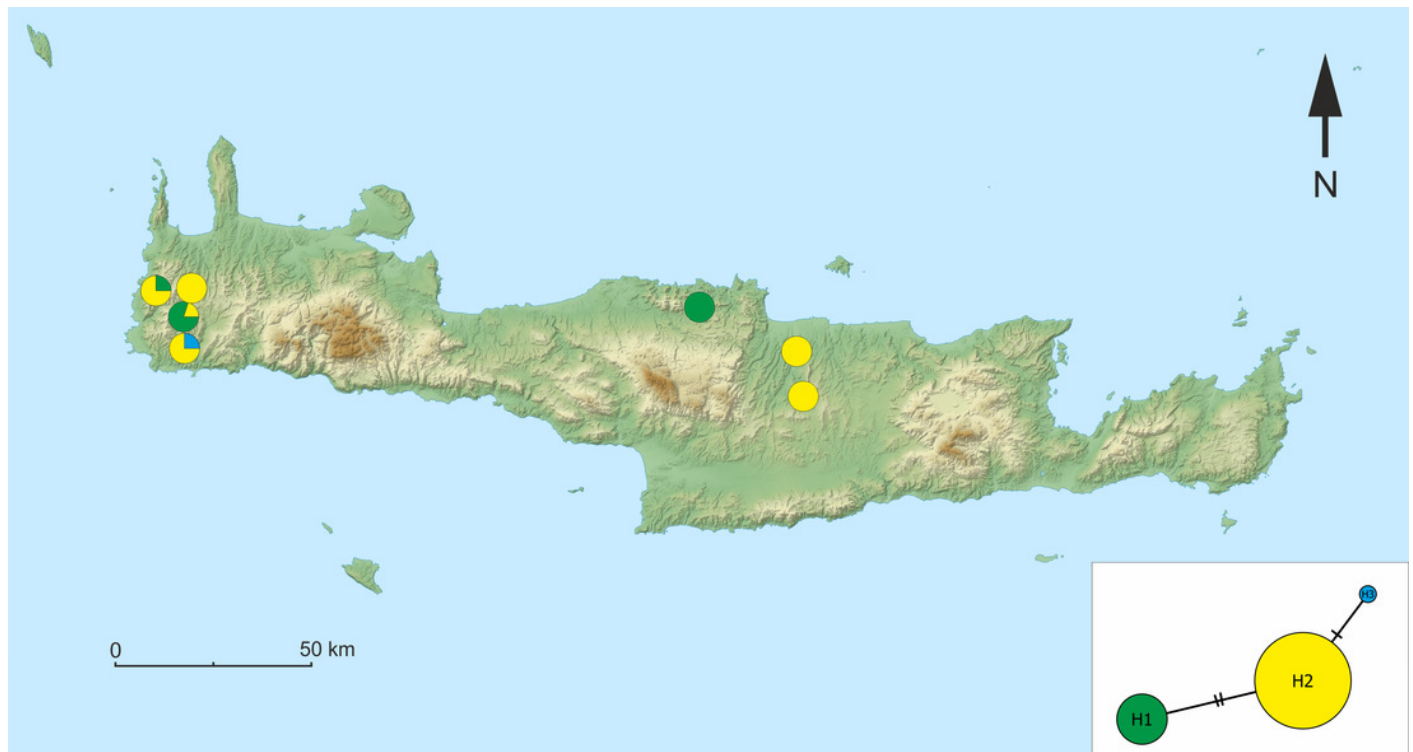
# Figure 8

Neighbor-joining tree of the *Gammarus plaitisi* sp. nov. with members of *Gammarus* cf. *pulex*, obtained from our data and mined from NCBI GenBank with the addition of the outgroups.

The numbers by respective nodes indicate bootstrap values ≥ 0.75. The scale bar corresponds to the number of substitutions per site. The rows of respective bars represent the delimitation of molecular operational taxonomic units (MOTU) by various methods of species delimitation.
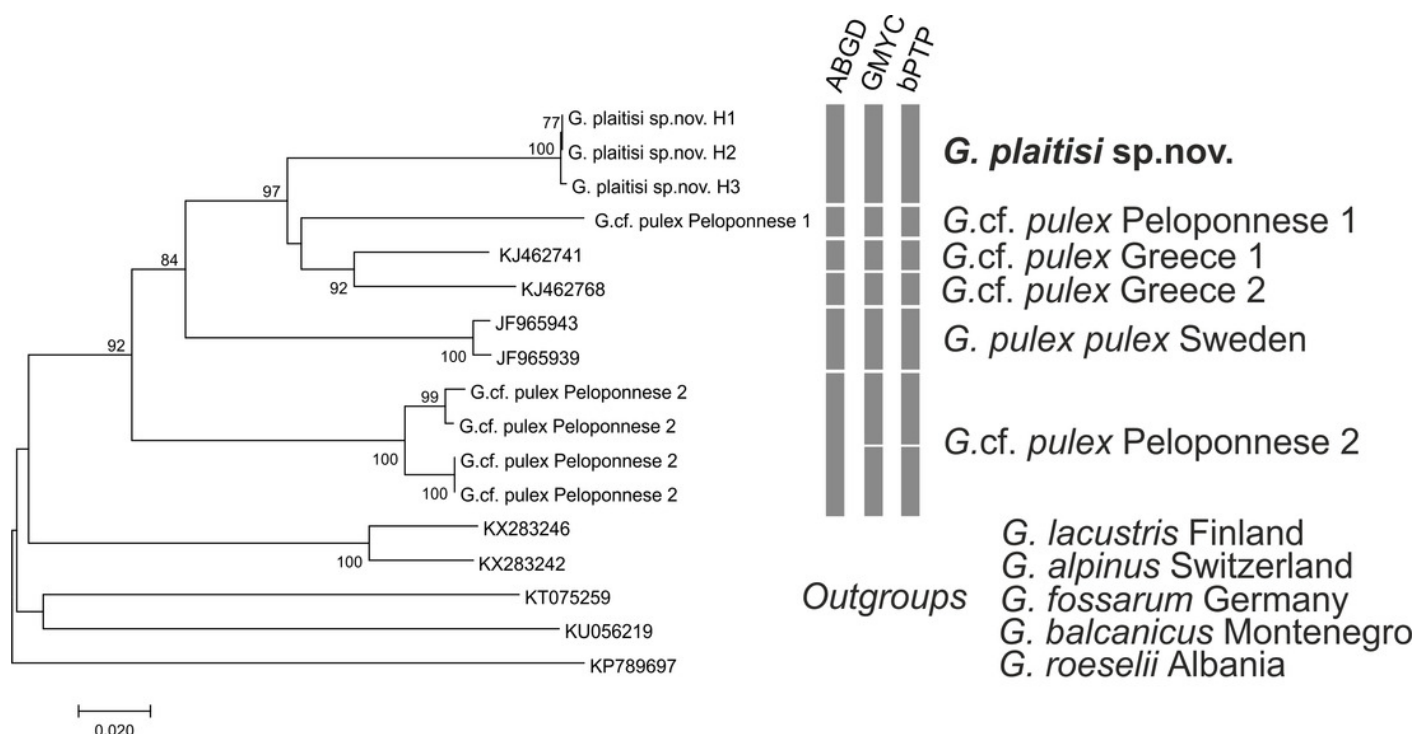
# Figure 9

Maximum clade credibility, time-calibrated Bayesian reconstruction of phylogeny of the *Gammarus plaitisi* sp. nov. with members of *Gammarus* cf. *pulex* from Peloponnese and Northern Greece.

Phylogeny was inferred from sequences of the mitochondrial COI and 16S genes and nuclear 28S, ITS1 and EF1-α genes. The numbers by respective nodes indicate Bayesian posterior probability values ≥ 0.85. Grey bars indicate the respective MOTUs of *Gammarus* morphospecies and grey node bars represent 95% HPD.
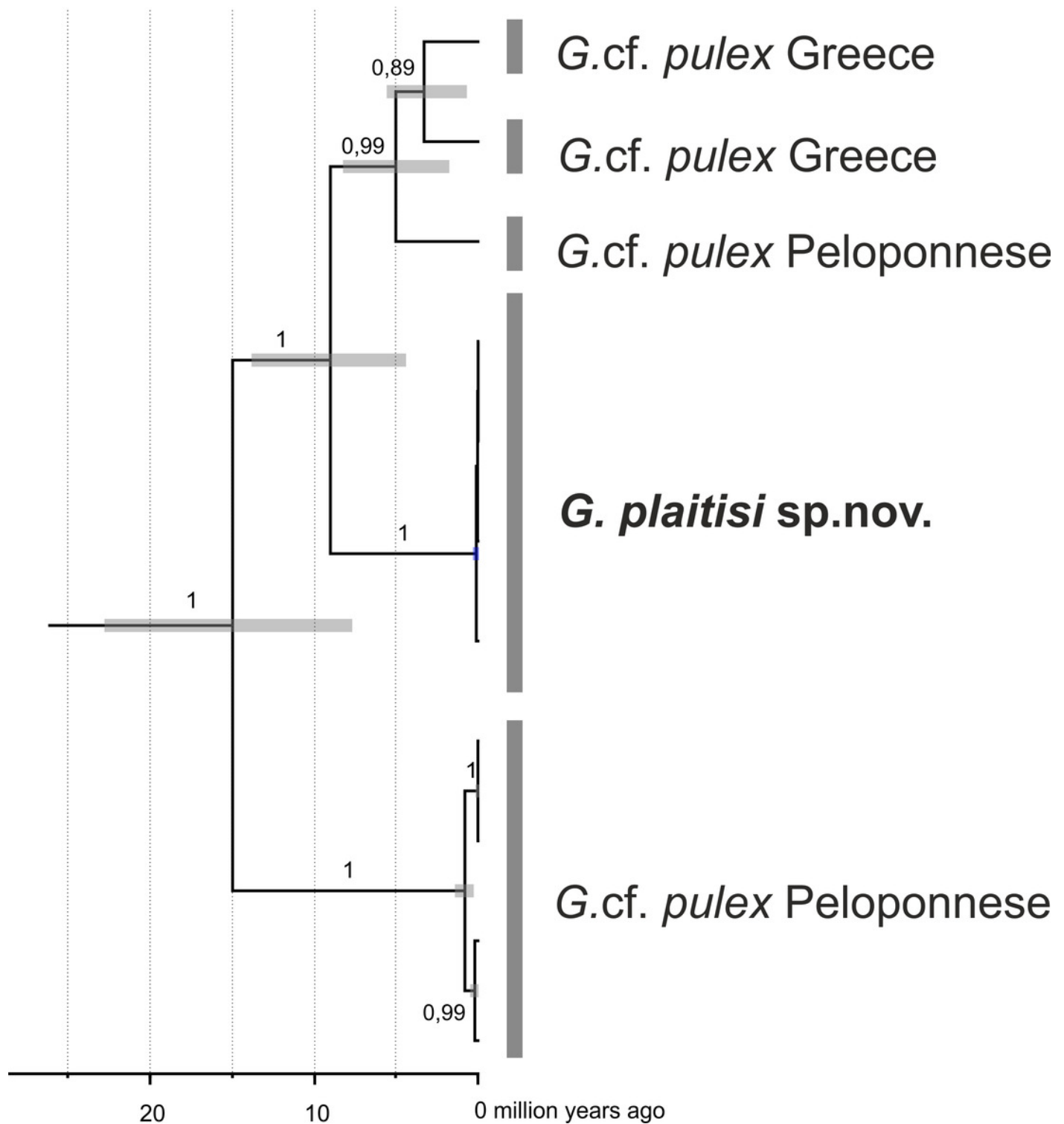
Material of *Gammarus* cf. *pulex* and outgroups used in our study.

1    Tab.1 Material of *Gammarus* cf. *pulex* and outgroups used in our study.

| MOTU | Locality | N | Accession number | Reference |
|---|---|---|---|---|
| G.pulex pulex | Sweden, Uppsala | 1 | JF965943 | Hou et al. 2011 |
| G.pulex pulex | Sweden | 1 | JF965939 | Hou et al. 2011 |
| G.cf pulex Greece 1 | Northern Greece | 2 | KJ462741 | Wysocka et al. (2014) |
| G.cf pulex Greece 2 | | | KJ462768 | |
| G.cf pulex Peloponnese 1 | Northern Peloponnese | 5 | MG784489 | This study |
| G.cf pulex Peloponnese 2 | | | MG784478 | This study |
| | | | MG784486 | This study |
| | | | MG784481 | This study |
| | | | MG784485 | This study |
| G.fossarum | Germany: North Rhine-Westphalia | 1 | KT075259 | Grabner et al. (2015) |
| G.lacustris | Finland: Jaekaelaevuoma | 1 | KX283246 | Alther et al. (2016) |
| G.alpinus | Switzerland: Lai da Palpuogna | 1 | KX283242 | Alther et al. (2016) |
| G.balcanicus | Montenegro | 1 | KU056219 | Mamos et al. (2016) |
| G.roeselii | Albania: Lake Shkodra | 1 | KP789697 | Grabowski et al. (2017a) |

Results of cross-validation of three substitution rates used in Bayesian analyses.

Tab.2 Results of cross-validation of three substitution rates used in Bayesian analyses.

| Node | Rate 0.0113 | Rate 0.0115 | Rate 0.0129 |
|---|---|---|---|
| *Gammarus plaitisi* divergence from closest *G*.cf *pulex* | 9.4 [4.8-14.1] | **9.2 [4.6-13.8]** | 8.2 [4.1-12.8] |

Material of *Gammarus plaitisi* sp.nov used in this study.

Tab.3 Material of *Gammarus plaitisi* sp.nov used in this study.

| Site | Coordinates | N | Haplotype counts |
|------|-------------|---|------------------|
| PC13 (spring in Sfinari beach) | 35.41533, 23.56127 | 4 | H2 (3), H1 (1) |
| PC14 (stream near Elos) | 35.36567, 23.63718 | 5 | H1 (4), H2 (1) |
| PC17 (Pelekaniotikos river) | 35.30729, 23.63583 | 4 | H2 (3), H3 (1) |
| PC22 (spring near Vlatos) | 35.39724, 23.65512 | 4 | H2 (4) |
| KPM22 (springs in Nikos Kazantzakis) | 35.19084, 25.22233 | 15 | H2 (15) |
| KPM23 (stream 8km from Iraklion) | 35,28893, 25,20423 | 7 | H2 (7) |
| KPM33 (Fodele, locus typicus) | 35.37828, 24.95833 | 4 | H1 (4) |